Logarithmic singularities and quantum oscillations in magnetically doped topological insulators

D. Nandi,[1] Inti Sodemann,[2,3] K. Shain,[1] G. H. Lee,[1,4] K.-F. Huang,[1] Cui-Zu Chang,[5,6] Yunbo Ou,[5] S. P. Lee,[7,8] J. Ward,[1] J. S. Moodera,[5] P. Kim,[1] and A. Yacoby[1,*]

[1]*Department of Physics, Harvard University, Cambridge, Massachusetts 02138, USA*
[2]*Max-Planck Institute for the Physics of Complex Systems, D-01187 Dresden, Germany*
[3]*Department of Physics, Massachusetts Institute of Technology, Cambridge, Massachusetts 02139, USA*
[4]*Department of Physics, Pohang University of Science and Technology, Pohang 790-784, Republic of Korea*
[5]*Francis Bitter Magnet Lab, Massachusetts Institute of Technology, Cambridge, Massachusetts 02139, USA*
[6]*Center for Nanoscale Science and Department of Physics, Pennsylvania State University, University Park, Pennsylvania 16802-6300, USA*
[7]*Department of Physics, University of Alberta, Edmonton, Alberta, Canada T6G 2E1*
[8]*Department of Physics and Astronomy, John Hopkins University, Baltimore, Maryland 21218, USA*

(Received 4 December 2017; published 26 February 2018)

We report magnetotransport measurements on magnetically doped $(Bi,Sb)_2Te_3$ films grown by molecular beam epitaxy. In Hall bar devices, we observe logarithmic dependence of transport coefficients in temperature and bias voltage which can be understood to arise from electron-electron interaction corrections to the conductivity and self-heating. Submicron scale devices exhibit intriguing quantum oscillations at high magnetic fields with dependence on bias voltage. The observed quantum oscillations can be attributed to bulk and surface transport.

DOI: 10.1103/PhysRevB.97.085151

I. INTRODUCTION

Breaking of time-reversal symmetry in topological insulators can unlock exotic phenomenon such as the quantized anomalous Hall effect [1–5], giant magneto-optical Kerr and Faraday effects [6], the inverse spin-galvanic effect [7], the image magnetic monopole effect [8], and chiral Majorana modes [9,10]. Angle-resolved photoemission spectroscopy measurements have revealed the presence of a magnetic gap at the Dirac point as well as hedgehog spin texture in magnetic topological insulators [11,12]. Proximity coupling to a magnetic insulator such as EuS, yttrium iron garnet, and thulium iron garnet [13–15] or introducing magnetic dopants like Mn, Cr, and V [2,3,16] can remove time-reversal symmetry. Such efforts have induced long-range ferromagnetic order in topological insulators.

In this paper we explore magnetotransport in magnetically doped ultrathin films of $(Bi,Sb)_2Te_3$ to understand the role of different scattering mechanisms. By studying the effect of temperature and voltage bias on the longitudinal and anomalous Hall resistances, we observe logarithmic dependencies on temperature and voltage bias. Joule heating due to voltage bias increases the effective temperature of the hot electrons [17]. The logarithmic singularities are originating from the interplay of electron-electron interaction and disorder. We find that our observed logarithmic corrections quantitatively agree with the Alshuler-Aranov theory of electron-electron interactions. Furthermore, in submicron-sized mesocale devices we observe quantum oscillations that depend on voltage bias and weaken with increasing sample width.

II. MATERIALS AND METHODS

The four-quintuple-layer (QL)-thick pristine and V-doped $(Bi,Sb)_2Te_3$ films were grown on $SrTiO_3$ (111) substrate by molecular beam epitaxy. The growth process was monitored *in situ* by reflection high-energy electron diffraction to ensure high-quality films [3,18,19]. To prevent oxidation, a capping layer of 10-nm tellurium was deposited. The devices were fabricated employing standard photolithography and electron-beam lithography techniques. The device schematic and optical image of a Ti/Nb/NbN contacted magnetic topological insulator film is shown in Figs. 1(a) and 1(b). The transport measurements were done in a ^{3}He-^{4}He dilution refrigerator using standard ac lock-in measurement techniques. Here we summarize results from a pristine Hall bar device, H_0; a V-doped Hall bar device, H_1; and a V-doped submicron scale device, D_1.

III. RESULTS AND DISCUSSION

Magnetotransport measurements in a Hall bar device, H_0, on pristine four-QL-thick $(Bi,Sb)_2Te_3$ films presented in Fig. 2(a) exhibit a dip in the longitudinal resistance R_{xx} at $B = 0$ T which is attributed to a weak antilocalization effect [20,21]. This is because in the presence of strong spin-orbit coupling time-reversed trajectories have opposite spin orientations which lead to a destructive interference and a resistance minimum [22].

We measured the bias dependence of the longitudinal resistance R_{xx} in the same device. The results are shown in Figs. 2(b) and 2(c) for a few different magnetic fields and exhibit a logarithmic dependence on voltage bias. Weak antilocalization is in itself a possible cause of logarithmic correction. However lowering the temperature or voltage bias is expected to make the weak antilocalization effect more

*yacoby@physics.harvard.edu

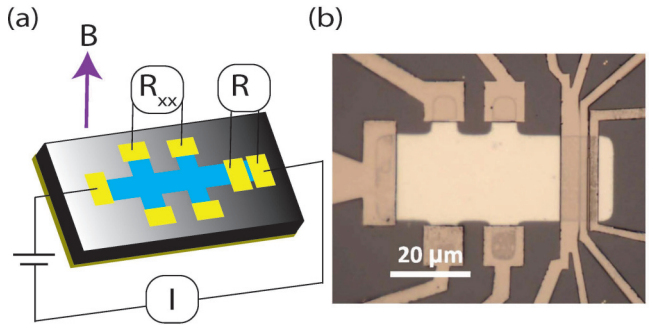

FIG. 1. (a) Schematics of a magnetic topological insulator device. (b) Optical image of a Hall bar device, H_1, and a two terminal device, D_1, simultaneously patterned on magnetically (vanadium) doped topological insulators.

pronounced thereby decreasing resistivity, which is inconsistent with Figs. 2(b) and 2(c).

Further by introducing magnetic impurities, the weak antilocalization effects can be heavily suppressed as has been reported in Fe-doped Bi_2Te_3 and Cr-doped Bi_2Se_3 films

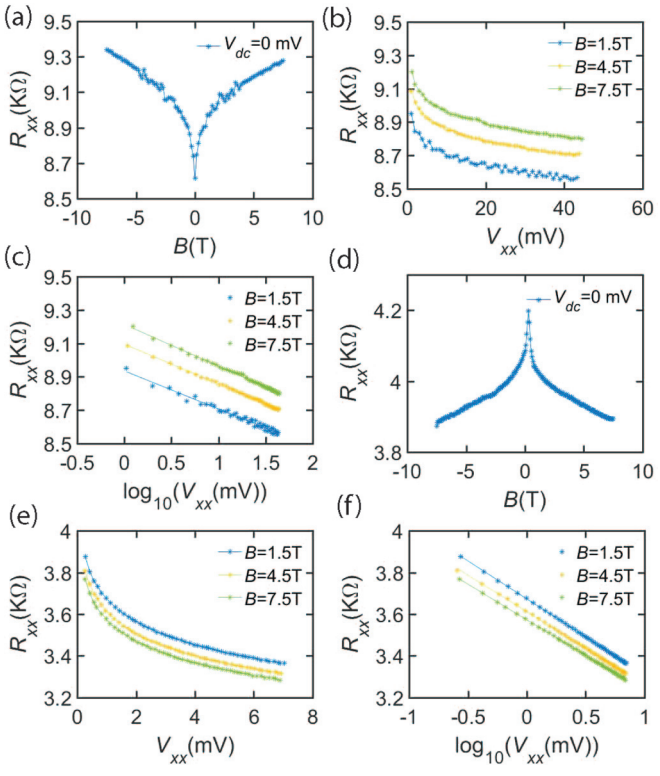

FIG. 2. Comparison of magnetotransport in pristine and V-doped four-QL-thick $(Bi,Sb)_2Te_3$ films. (a) Magnetoresistance dip at $B = 0$ T in the sweep range $B = -7.5$ to $+7.5$ T for pristine $(Bi,Sb)_2Te_3$ samples. (b) Bias dependence of pristine $(Bi,Sb)_2Te_3$ film at $B = 1.5$, 4.5, and 7.5 T. (c) Logarithmic plot for bias dependence of four-QL pristine $(Bi,Sb)_2Te_3$ film at $B = 1.5$, 4.5, and 7.5 T. (d) Magnetoresistance peak at $B = 0$ T in the sweep range $B = -7.5$ to $+7.5$ T for V-doped $(Bi,Sb)_2Te_3$. (e) Bias dependence of V-doped $(Bi,Sb)_2Te_3$ film at $B = 1.5$, 4.5, and 7.5 T. (f) Logarithmic plot for bias dependence of V-doped $(Bi,Sb)_2Te_3$ film at $B = 1.5$, 4.5, and 7.5 T.

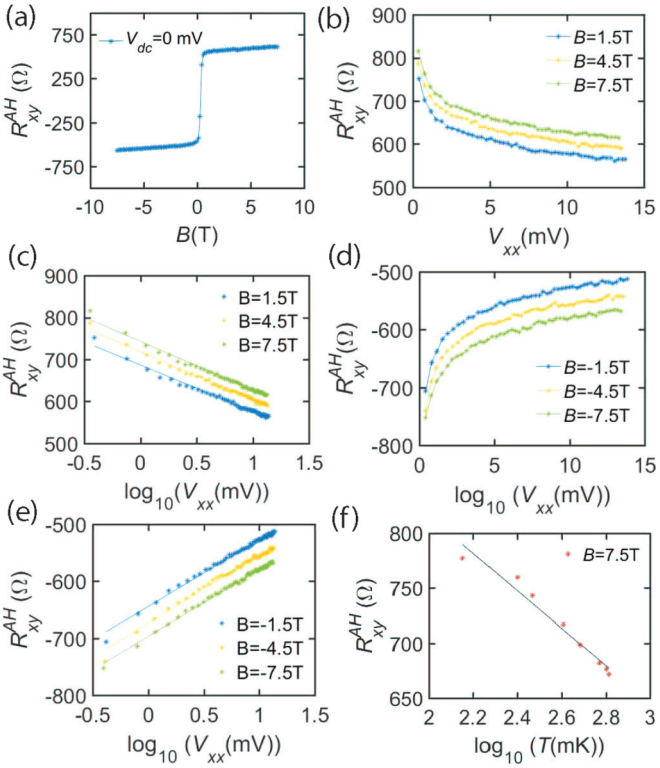

FIG. 3. Voltage bias and temperature dependence of the anomalous Hall effect of V-doped four-QL-thick $(Bi,Sb)_2Te_3$ films. (a) Magnetic field dependence of the anomalous hall resistance R_{xy}^{AH} measured at $V_{dc} = 0$. (b) Bias dependence of R_{xy}^{AH} at $B = 1.5, 4.5$, and 7.5 T. (c) Logarithmic plot for bias dependence of R_{xy}^{AH} at $B = 1.5, 4.5$, and 7.5 T. (d) Bias dependence of R_{xy}^{AH} at $B = -1.5, -4.5$, and -7.5 T. (e) Logarithmic plot for bias dependence of R_{xy}^{AH} at $B = -1.5, -4.5$, and -7.5 T. (f) R_{xy}^{AH} exhibits a logarithmic dependence on temperature at $B = 7.5$ T in the temperature range of 140 to 650 mK.

[23–25]. Figure 2(d) shows the magnetoresistance in a V-doped $(Bi,Sb)_2Te_3$ film has a peak instead of a dip at $B = 0$ T as seen in pristine samples. Even when the weak antilocalization effects are suppressed, the longitudinal resistance R_{xx} in a V-doped $(Bi,Sb)_2Te_3$ film has a logarithmic dependence on voltage bias as shown in Figs. 2(e) and 2(f) at different magnetic fields.

Weak localization in disordered two-dimensional (2D) systems is also a potential explanation for a logarithmic increase in resistance at low temperatures. The existence of weak localization relies on the existence of coherent constructive interference of time-reversed trajectories for an electron to return to the origin [26]. Moderate external magnetic fields as well as magnetic impurities, which break time-reversal symmetry, are typically enough to suppress logarithmic corrections arising from weak localization [27–29]. However, the logarithmic corrections observed in our experiments persist even at fields of 7.5 T.

A way to identify logarithmic corrections due to weak localization is by the absence of logarithmic corrections to R_{xy} [27,28,30]. In Fig. 3(a) anomalous Hall measurements are shown without an applied bias. The R_{xy}^{AH} jumps at the coercive field when the magnetization switches its direction. Figures 3(b) and 3(c) show that the logarithmic dependence

on voltage bias is present in the anomalous Hall resistance R_{xy}^{AH} as well. The data are antisymmetric in the magnetic field as shown in Figs. 3(d) and 3(e); therefore we can rule out spurious R_{xx} contributions. Interestingly, if instead of bias voltage the temperature of the sample is changed, a similar decrease in the anomalous Hall resistance R_{xy}^{AH} is observed as shown in Fig. 3(f). Therefore, weak localization cannot explain the transport behavior that we observe.

Logarithmic corrections to conductance could also arise from scattering off magnetic impurities as in the Kondo effect [31–33]. However, in the ferromagnetic state magnetic spin-flips should become increasingly energetically unfavorable at low temperatures and at large external magnetic fields. More importantly, the fact that logarithmic dependencies are also observed in topological insulator thin films in the absence of magnetic dopants [34,35] makes this scenario an unlikely explanation of our findings.

Magnetotransport studies in pristine topological insulator Bi_2Se_3 films found it crucial to include electron-electron interactions [34,35]. We explain why the observed logarithmic singularities are due to electron-electron interactions in the 2D surface states. As first realized by Altshuler and Aronov [36] (AA), disordered 2D electron systems exhibit a breakdown of the Fermi-liquid theory due to reduced ability of the disordered electron gas to screen the Coulomb interaction. The logarithmic corrections in the AA theory are pervasive and are expected to arise not only in transport properties but also in equilibrium thermodynamic quantities such as specific heat [28]. One of the key differences of the AA corrections with those in the localization theory is that both the longitudinal and Hall resistivities are expected to acquire logarithmic corrections [27,28]. In fact the logarithmic corrections are most easily expressed in terms of conductivities rather than resistivities in the AA theory, because the Hall conductivity is expected to remain unchanged. Specifically one expects the logarithmic corrections in the AA model to be given by [27–29]

$$\delta\sigma_{xx}(\varepsilon) = \kappa\frac{e^2}{h}\log\left(\frac{\varepsilon\tau}{\hbar}\right), \quad \delta\sigma_{xy} = 0, \tag{1}$$

where τ is the elastic scattering time and ε is an appropriate energy scale that can be chosen to be the largest among the temperature k_BT or the frequency $\hbar\omega$, at which the conductivity is probed. κ is a dimensionless number that takes different values for spinless and spinful electrons, and it depends on a dimensionless parameter F that characterizes a Hartree contribution to the conductivity corrections [28,29,37]. This parameter takes the following forms for spinless and spinful electrons:

$$\kappa^{\mathrm{spinless}} = \frac{1}{2\pi}, \tag{2}$$

$$\kappa^{\mathrm{spinfull}} = \frac{1}{2\pi}(2-2F), \tag{3}$$

For short-range interaction, $F = 1$, and for long-range interaction, $F = 0$ [38]. For spin-split bands one expects that for a spin splitting $\Delta \gg k_BT$, the only singular logarithmic terms arise from exchange and $S_z = 0$ Hartree contributions, and the

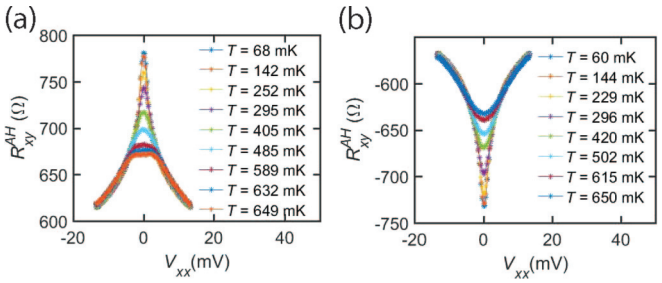

FIG. 4. Voltage bias dependence of the anomalous Hall effect at several fixed temperatures in V-doped four-QL-thick $(Bi,Sb)_2Te_3$ films for (a) $B = 7.5$ T and (b) $B = -7.5$ T.

expression for κ is [28]

$$\kappa^{\text{spin-split}} = \frac{1}{2\pi}(2-F) \approx 0.32\left(1-\frac{1}{2}F\right). \tag{4}$$

Our magnetic samples are expected to be spin-split, whereas the precise level of spin polarization is unknown to us [28,29].

Figures 4(a) and 4(b) further explore the dependence of the anomalous Hall effect on both voltage bias and temperature. Increasing either voltage or temperature lowers the anomalous Hall resistance which supports a self-heating mechanism due to applied bias.

We believe that the origin of the non-Ohmic behavior we observe, namely the logarithmic dependence of the conductivity on voltage bias, is fundamentally no different than the logarithmic dependence on temperature and can be understood simply as a consequence of Joule heating. In other words, as the electrons are accelerated by the electric field they inevitably gain energy, and, once they reach a steady state of current flow, this inevitably implies that the electrons possess a larger effective temperature compared to that of the lattice or other reservoirs that serve as heat sinks. By appealing to a simple model of Joule heating [39] one can effectively replace the argument of the logarithm in Eq. (1) by $\varepsilon \sim \max(AV^{2/(2+p)}, K_BT, \hbar\omega)$, where V is the voltage bias that drives the transport, A is a constant, and p is the power that controls the temperature dependence of the electron's inelastic scattering rate, $\tau_{\mathrm{in}} \propto T^{-p}$. The logarithmic fits of the Hall resistivity vs temperature have approximately twice the slope of those of the Hall resistivity vs the bias voltage, indicating that $p \sim 2$, as shown in Fig. 5.

The Joule heating induced by the bias voltage proves to be a more efficient way to tune the electron temperature than the direct control of the temperature of the sample, and hence we focus on this dependence for the remainder of the discussion. The expected behavior of the correction to the conductivity for low-temperature dc measurements from the AA theory as a function of voltage is

$$\delta\sigma_{xx}(V) = \frac{2\kappa}{(2+p)}\frac{e^2}{h}\log(V), \quad \delta\sigma_{xy}(V) = 0. \tag{5}$$

From the data, σ_{xx} and σ_{xy} are calculated using the relations

$$\sigma_{xx} = \frac{\rho_{xx}}{\rho_{xy}^2+\rho_{xx}^2}, \quad \sigma_{xy} = \frac{\rho_{yx}}{\rho_{xy}^2+\rho_{xx}^2}, \tag{6}$$

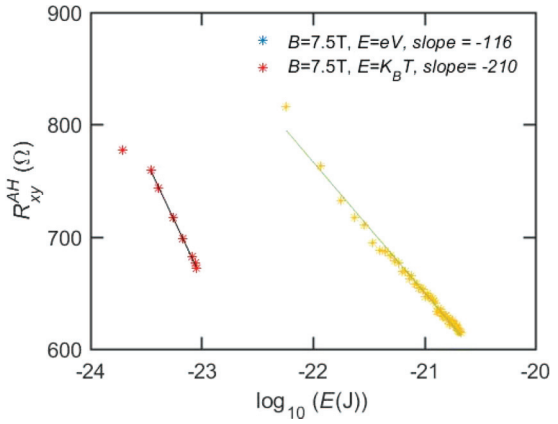

FIG. 5. Comparison of the dependence of the anomalous Hall resistance R_{xy}^{AH} on the logarithm of $K_B T$ and eV in V-doped four-QL-thick $(Bi,Sb)_2Te_3$ films at $B = 7.5$ T.

where ρ_{xx} and ρ_{xy} are the resistivities considering the square-shaped sample geometry. As illustrated in Fig. 6(a) our data are consistent with logarithmic corrections in σ_{xx} while there are no apparent logarithmic corrections in σ_{xy}, as expected from the AA theory. The anomalous Hall conductivity is nearly quantized at $\pm e^2/h$ as shown in Fig. 6(b). Anecdotally, we

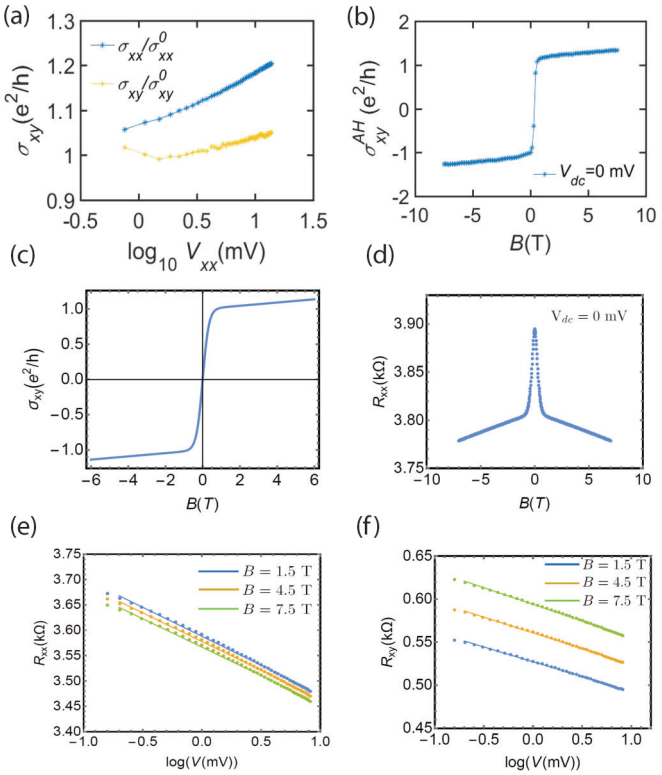

FIG. 6. Transport coefficients in the V-doped Hall bar (device H_1) as a function of bias. (a) Logarithmic plot for σ_{xx} (blue) and σ_{xy} (orange) at $B = 1$ T. (b) Magnetic field dependence of σ_{xy} at $V_{dc} = 0$. (c) and (d) Theoretical model of the magnetic field dependence of σ_{xy} and R_{xx}. (e) and (f) Simulation of the dependence of R_{xx} and R_{xy} on bias at $B = 1.5, 4.5$, and 7.5 T as expected from interaction corrections in disordered 2D films.

argue that quantization of $\sigma_{xy}^{\mathrm{AH}}$ is less sensitive to finite bulk carriers than R_{xy}^{AH}.

To quantify the logarithmic behavior we fit the voltage-dependent nonlinear conductivity as (expressing bias in volts)

$$\sigma_J(V) = \sigma_J^0 + \delta\sigma_J \log(V),\ J = \{xx, xy\}. \tag{7}$$

We obtain $\sigma_{xx}^0 \approx 9.17e^2/h$ and $\delta\sigma_{xx} \approx 0.33e^2/h$, and $\sigma_{xy}^0 \approx 1.58e^2/h$ and $\delta\sigma_{xy} \approx 0.02e^2/h$. Notice the smallness of the bias dependence of σ_{xy} compared to that of σ_{xx}. Therefore, considering that it is possible that small systematic errors can arise from the mixing of R_{xx} and R_{xy} (e.g., if contacts are slightly misaligned R_{xy} picks a small contribution from R_{xx}), we conclude that our data are consistent with σ_{xy} with negligible logarithmic bias dependence and while having significant logarithmic bias dependence on σ_{xx}, as expected from the AA theory. We observe, however, an interesting quantitative deviation from the expectation of the AA theory. Using the approximate value of $p \sim 2$, obtained by comparing the temperature and the voltage fits (see Fig. 5), the fitted parameter κ reads as

$$\pi\kappa_{\mathrm{fit}} \sim 2. \tag{8}$$

However, from Eqs. (2)–(4), we expect $\pi\kappa \leqslant 1$, under the natural assumption of repulsive interactions $F > 0$. The origin of this discrepancy is at present unknown to us, but we wish to remind the reader that the equations of the AA theory we have employed were derived for parabolic electrons without Berry phase effects, and it remains to be determined whether nontrivial orbital coherences, such as those giving rise to Berry curvatures for the bands of interest here, affect in any way the classic results of the AA theory.

A simple modeling of the resistivity can be done by using the expected conductivity behavior from the AA theory. The resistivity is taken to be of the form $\sigma_{xx} = \sigma_{xx}^0 + \delta\sigma_{xx}^0 \log(|V| + V_0)$, where $V_0 \sim 0.4$ mV is essentially a cutoff of the logarithm at small bias (which is controlled by the temperature scale T_0 and the constant A in the Joule heating model), and σ_{xx}^0 and $\delta\sigma_{xx}^0$ are field- and bias-independent quantities obtained by linear fitting of the logarithmic plots of the conductivity [40]. We add a simple description of the anomalous hall effect in which the Hall conductivity has a jump of e^2/h near the zero applied magnetic field in addition to the usual linear term reflecting the classical Hall effect. σ_{xy} in the model is presented in Fig. 6(c) and has the form $\sigma_{xy} = \frac{e^2}{h}\tanh(B/B_0) + \delta\sigma_{xy}^0 B$, where $B_0 \sim 0.3$ T reflects broadening of the jump of the magnetization as a function of field and $\delta\sigma_{xy}^0$ is field and bias independent. The model is able to reproduce the essential behavior of the resistivities and it is shown in Figs. 6(d)–6(f).

The transport results discussed above are for larger Hall bar ($\sim$20 μm) samples. Interestingly, when the device dimension was reduced to submicron range, prominent Shubnikov-de Haas (SdH) oscillations were observed. For example, in a 0.2-μm-wide device (device D_1) measured by two terminals, the oscillations were periodic in $1/B$ and had a nontrivial dependence on bias voltage. These quantum oscillations were seen in multiple samples with Ti/Nb/NbN and Ti/Al contacts. In particular, the zero bias minima turn into maxima in resistance at large voltage bias as shown in Fig. 7.

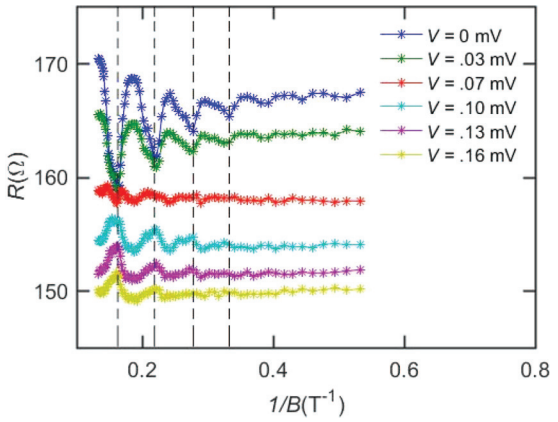

FIG. 7. Voltage bias dependence of quantum oscillations from magnetoresistance in the V-doped $(Bi,Sb)_2Te_3$ device D_1 of width $W = 0.2\ \mu$m.

We also studied the effect of temperature on the magneto-oscillations as shown in Fig. 8. The amplitude of the quantum oscillations is found to decrease with an increase in temperature. However, the transition from maxima to minima could not be observed at temperatures accessible in the dilution fridge. The inferred electron density is 9×10^{11} cm^{-2} (4.5×10^{11} cm^{-2}) for spinful (spinless) Fermions. The period of the SdH could not be changed by applying a back gate or a top gate. The screening of the top and bottom gates by the surface states results in the inability to change the Fermi energy of the bulk states as has been observed in other topological materials [41]. An estimate of the electron gas mobility is made from the onset magnetic field of the SdH oscillations $\mu_q \approx \frac{1}{B_q} \approx 6000$ cm^2 V^{-1} s^{-1} for the 200-nm-wide device [42]. This mobility is intriguingly large compared to macroscopic samples.

We describe a transport model for the nontrivial dependence of the quantum oscillations on voltage bias that we have observed in the narrow junctions. We assume the magneto-conductance to be given by

$$g(B,V) = g_0 + \alpha\rho(\epsilon_F,B)\ln(\varepsilon\tau/\hbar), \tag{9}$$

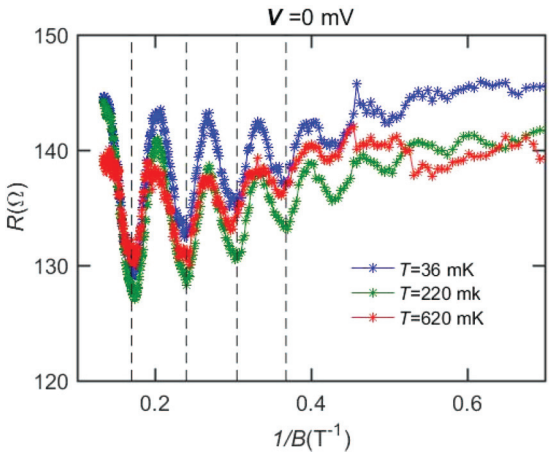

FIG. 8. Temperature dependence of quantum oscillations from magnetoresistance in the V-doped $(Bi,Sb)_2Te_3$ device D_1 of width $W = 0.2\ \mu$m.

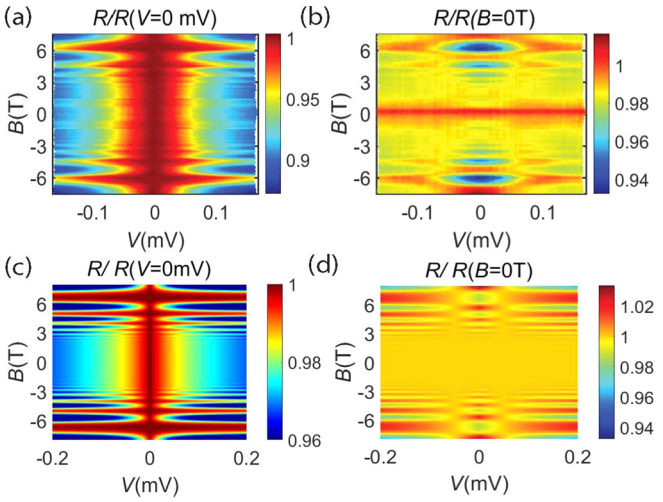

FIG. 9. (a) and (b) The resistance in the V-doped $(Bi,Sb)_2Te_3$ device D_1 is normalized to its zero bias value and normalized to its zero magnetic field value, respectively. The evolution is studied with magnetic field and applied bias voltage. The SdH oscillations are present both at small and large bias voltages. However, the zero bias maxima become minima at large bias voltages at a fixed magnetic field and vice versa. (c) A model with two conduction mechanisms in parallel that incorporates logarithmic decay with the applied bias of the SdH oscillations on top of a constant background conduction. The resistance is normalized to the zero bias value for comparison to the experimental data. (d) The two-conduction-mechanism model captures the evolution from maxima to minima of the resistance normalized to the zero magnetic field value with voltage bias.

where g_0 is assumed to be a constant background conduction and $\rho(\epsilon_F,B)$ is the SdH density of states given by

$$\rho(\epsilon_F,B) = \frac{2eB}{h}\sum_{j=0}^{j=\infty}\frac{1}{(2\pi)^{1/2}\Gamma}\exp\left(-\frac{(\epsilon_F-\epsilon_j)^2}{2\Gamma^2}\right), \tag{10}$$

where Γ is the half-width of Landau level broadening and ϵ_j is the single-particle Landau level energy [43]. The presence of both bulk and surface conduction mechanisms in topological insulators has been found previously [44–49]. Figures 9(a) and 9(b) display the magnetotransport data normalized to zero bias and zero magnetic field. Similarly, in the model, the resistance $r(B,V) = 1/g(B,V)$ is normalized to its value at zero bias voltage and the magnetic field as is shown in Figs. 9(c) and 9(d), respectively.

While we do have an understanding of the voltage dependence of the oscillations, there are properties that are less well understood. The contrast of the quantum oscillations is found to decrease systematically with increasing width. Such dependence of the visibility of quantum oscillations on the channel width is unusual. The quantum oscillations are discussed in further detail in the Supplemental Material [40].

IV. CONCLUSION

We have studied magnetotransport in V-doped $(Bi,Sb)_2Te_3$ and have found logarithmic singularities in the longitudinal resistance R_{xx} and the anomalous Hall resistance R_{xy}^{AH} which is well explained quantitatively by quantum corrections due

to electron-electron interactions. In submicron scale devices, SdH oscillations are observed where the maxima transition to minima with voltage bias. A simple transport model explains these observations.

ACKNOWLEDGMENTS

The authors acknowledge insightful discussions with Ashwin Viswanathan, Liang Fu, Brian Skinner, Toeno Vander Saar, Lucas Orona, and Anindya Das. The authors are grateful to Di S. Wei, Tony X. Zhou, Pat Gunman, and Andrei Levin for invaluable help with developing the sample fabrication. A.Y., D.N., K.S., and J.W. acknowledge support from Gordon and Betty Moore Foundation Grant No. 4531, ARO Grant No. W 911 NF-16-1-0491, DOE Grant No. DE-SC0001819, and ARO Grant No. W911NF-17-1-0023. A.Y. also acknowledges support in part by the U.S. Army Research Laboratory and the U.S. Army Research Office under Grant No. W911NF-16-1-0491. I.S. acknowledges support from an MIT Pappalardo Fellowship. P.K., G.H.L., and K.F.H. acknowledge support from NSF Grant No. DMR-1420634. J.S.M., C.Z.C. and Y.O. acknowledge support from NSF Grant No. DMR-1700137 and ONR Grant No. N00014-16-1-2657.

[1] R. Yu, W. Zhang, H. J. Zhang, S. C. Zhang, X. Dai, and Z. Fang, Science **329**, 61 (2010).
[2] C. Z. Chang, J. Zhang, X. Feng, J. Shen, Z. Zhang, M. Guo, K. Li, Y. Ou, P. Wei, L. L. Wang *et al.*, Science **340**, 167 (2013).
[3] C. Z. Chang, W. Zhao, D. Y. Kim, H. Zhang, B. A. Assaf, D. Heiman, S. C. Zhang, C. Liu, M. H. W. Chan, and J. S. Moodera, Nat. Mater. **14**, 473 (2015).
[4] M. Mogi, R. Yoshimi, A. Tsukazaki, K. Yasuda, Y. Kozuka, K. S. Takahashi, M. Kawasaki, and Y. Tokura, Appl. Phys. Lett. **107**, 182401 (2015).
[5] C. Z. Chang, W. Zhao, D. Y. Kim, P. Wei, J. K. Jain, C. Liu, M. H. W. Chan, and J. S. Moodera, Phys. Rev. Lett. **115**, 057206 (2015).
[6] W. K. Tse and A. H. MacDonald, Phys. Rev. Lett. **105**, 057401 (2010).
[7] I. Garate and M. Franz, Phys. Rev. Lett. **104**, 146802 (2010).
[8] X. L. Qi, R. Li, J. Zang, and S. C. Zhang, Science **323**, 1184 (2009).
[9] X. L. Qi, T. L. Hughes, and S. C. Zhang, Phys. Rev. B **82**, 184516 (2010).
[10] Q. L. He, L. Pan, A. L. Stern, E. C. Burks, X. Che, G. Yin, J. Wang, B. Lian, Q. Zhou, E. S. Choi *et al.*, Science **357**, 294 (2017).
[11] Y. L. Chen, J. H. Chu, J. G. Analytis, Z. K. Liu, K. Igarashi, H. H. Kuo, X. L. Qi, S. K. Mo, R. G. Moore, D. H. Lu *et al.*, Science **329**, 659 (2010).
[12] S. Y. Xu, M. Neupane, C. Liu, D. Zhang, A. Richardella, L. A. Wray, N. Alidoust, M. Leandersson, T. Balasubramanian, J. Sánchez Barriga *et al.*, Nat. Phys. **8**, 616 (2012).
[13] Z. Jiang, C. Z. Chang, C. Tang, P. Wei, J. S. Moodera, and J. Shi, Nano Lett. **15**, 5835 (2015).
[14] F. Katmis, V. Lauter, F. S. Nogueira, B. A. Assaf, M. E. Jamer, P. Wei, B. Satpati, J. W. Freeland, I. Eremin, D. Heiman *et al.*, Nature (London) **533**, 513 (2016).
[15] C. Tang, C. Z. Chang, G. Zhao, Y. Liu, Z. Jiang, C. X. Liu, M. R. McCartney, D. J. Smith, T. Chen, J. S. Moodera *et al.*, Sci. Adv. **3**, e1700307 (2017).
[16] Y. S. Hor, P. Roushan, H. Beidenkopf, J. Seo, D. Qu, J. G. Checkelsky, L. A. Wray, D. Hsieh, Y. Xia, S. Y. Xu, D. Qian, M. Z. Hasan, N. P. Ong, A. Yazdani, and R. J. Cava, Phys. Rev. B **81**, 195203 (2010).
[17] J. K. Viljas and T. T. Heikkilä, Phys. Rev. B **81**, 245404 (2010).
[18] M. Liu, W. Wang, A. R. Richardella, A. Kandala, J. Li, A. Yazdani, N. Samarth, and N. P. Ong, Sci. Adv. **2**, e1600167 (2016).
[19] N. Samarth, Nat. Mater. **16**, 1068 (2017).
[20] J. Chen, H. J. Qin, F. Yang, J. Liu, T. Guan, F. M. Qu, G. H. Zhang, J. R. Shi, X. C. Xie, C. L. Yang, K. H. Wu, Y. Q. Li, and L. Lu, Phys. Rev. Lett. **105**, 176602 (2010).
[21] S. P. Chiu and J. J. Lin, Phys. Rev. B **87**, 035122 (2013).
[22] S. Hikami, A. I. Larkin, and Y. Nagaoka, Prog. Theor. Phys. **63**, 707 (1980).
[23] H. T. He, G. Wang, T. Zhang, I. K. Sou, G. K. L. Wong, J. N. Wang, H. Z. Lu, S. Q. Shen, and F. C. Zhang, Phys. Rev. Lett. **106**, 166805 (2011).
[24] M. Liu, J. Zhang, C. Z. Chang, Z. Zhang, X. Feng, K. Li, K. He, L. L. Wang, X. Chen, X. Dai, Z. Fang, Q. K. Xue, X. Ma, and Y. Wang, Phys. Rev. Lett. **108**, 036805 (2012).
[25] H. Z. Lu, J. Shi, and S. Q. Shen, Phys. Rev. Lett. **107**, 076801 (2011).
[26] G. Bergmann, Phys. Rep. **107**, 1 (1984).
[27] B. L. Altshuler, D. E. Khmel'nitzkii, A. I. Larkin, and P. A. Lee, Phys. Rev. B **22**, 5142 (1980).
[28] P. A. Lee and T. V. Ramakrishnan, Rev. Mod. Phys. **57**, 287 (1985).
[29] B. L. Altshuler and A. G. Aranov, *Electron-Electron Interactions in Disordered Systems*, edited by A. L. Efros and M. Pollak (North-Holland, Amsterdam, 1985).
[30] H. Fukuyama, J. Phys. Soc. Jpn. **49**, 644 (1980).
[31] P. W. Anderson, Phys. Rev. **124**, 41 (1961).
[32] J. Kondo, Prog. Theor. Phys. **32**, 37 (1964).
[33] J. Appelbaum, Phys. Rev. Lett. **17**, 91 (1966).
[34] M. Liu, C. Z. Chang, Z. Zhang, Y. Zhang, W. Ruan, K. He, L. L. Wang, X. Chen, J. F. Jia, S.-C. Zhang *et al.*, Phys. Rev. B **83**, 165440 (2011).
[35] J. Wang, A. M. DaSilva, C. Z. Chang, K. He, J. K. Jain, N. Samarth, X. C. Ma, Q. K. Xue, and M. H. W. Chan, Phys. Rev. B **83**, 245438 (2011).
[36] B. L. Altshulerand A. G. Aronov, Solid State Commun. **30**, 115 (1979).
[37] B. L. Altshuler, A. G. Aronov, and D. E. Khmelnitsky, J. Phys. C **15**, 7367 (1982).
[38] B. L. Altshuler, A. G. Aronov, and P. A. Lee, Phys. Rev. Lett. **44**, 1288 (1980).
[39] E. Abrahams, P. W. Anderson, and T. V. Ramakrishnan, Philos. Mag. B **42**, 827 (1980).
[40] See Supplemental Material at http://link.aps.org/supplemental/10.1103/PhysRevB.97.085151 for the sample processing details and theoretical estimates of density are provided in the Supplemental Materials.

[41] D. M. Mahler, J. Wiedenmann, C. Thienel, F. Schmitt, C. Ames, R. Schlereth, P. Leubner, C. Brune, H. Buhmann, D. D. Sante, C. Gould, G. Sangiovanni, and L. W. Molenkamp (unpublished).

[42] X. Cui, G. H. Lee, Y. D. Kim, G. Arefe, P. Y. Huang, C. H. Lee, D. A. Chenet, X. Zhang, L. Wang, F. Ye *et al.*, Nat. Nanotechnol. **10**, 534 (2015).

[43] J. P. Eisenstein, H. L. Stormer, V. Narayanamurti, A. Y. Cho, A. C. Gossard, and C. W. Tu, Phys. Rev. Lett. **55**, 875 (1985).

[44] J. G. Analytis, R. D. McDonald, S. C. Riggs, J. H. Chu, G. S. Boebinger, and I. R. Fisher, Nat. Phys. **6**, 960 (2010).

[45] J. G. Analytis, J. H. Chu, Y. Chen, F. Corredor, R. D. McDonald, Z. X. Shen, and I. R. Fisher, Phys. Rev. B **81**, 205407 (2010).

[46] D. X. Qu, Y. S. Hor, J. Xiong, R. J. Cava, and N. P. Ong, Science **329**, 821 (2010).

[47] J. Xiong, Y. Luo, Y. H. Khoo, S. Jia, R. J. Cava, and N. P. Ong, Phys. Rev. B **86**, 045314 (2012).

[48] H. Cao, J. Tian, I. Miotkowski, T. Shen, J. Hu, S. Qiao, and Y. P. Chen, Phys. Rev. Lett. **108**, 216803 (2012).

[49] K. Saha and I. Garate, Phys. Rev. B **90**, 245418 (2014).